Intensity distribution properties of Gaussian vortex beam propagation in atmospheric turbulence*

Qian Xian-Mei(钱仙妹)†, Zhu Wen-Yue(朱文越), and Rao Rui-Zhong(饶瑞中)

Key Laboratory of Atmospheric Composition and Optical Radiation of Chinese Academy of Sciences, Anhui Institute of Optics and Fine Mechanics, Chinese Academy of Sciences, Hefei 230031, *China*

(Received 21 May 2014; revised manuscript received 11 October 2014; published online 10 February 2015)

By using wave optics numerical simulation, the intensity-hole effect, beam spreading and wandering properties of Gaussian vortex beam propagation in atmospheric turbulence are investigated quantitatively. It is found that an intensity hole in the center of the beam pattern appears gradually as a Gaussian vortex beam propagates. The size of the intensity hole increases with the increase of the topological charge of the vortex phase. However, the intensity hole could to some extent be filled with optical energy by atmospheric turbulence, especially in strong turbulence. The radius of the intensity hole first decreases and then increases with the growth of turbulence strength. The effective radius of vortex beam with larger topological charge is greater than with a smaller topological charge. But the topological charge has no evident influence on beam wandering.

Keywords: Gaussian vortex beam, intensity hole, beam spreading, beam wandering

PACS: 42.25.Bs, 42.25.Kb, 92.60.Ta, 92.60.hk **DOI:** 10.1088/1674-1056/24/4/044201

1. Introduction

Recently, much work has been done to investigate the properties of beams carrying phase vortices.[1–9] Such beams carry orbital angular momentum and can impart this angular momentum to microscopic particles. Consequently, vortex beams have been studied for use as optical spanners and tweezers.[10,11] Another important feature of a vortex beam is that the topological charge of the vortex phase is a discrete variable and is stable under phase perturbation. This suggests that the phase topological charge could be utilized as an information carrier in free-space optical communications. However, for free-space optical communications, the laser beam should propagate through a turbulent atmosphere to transmit information to the receiver. The atmospheric turbulence may reduce the coherence of the source beam and then restrict the performance of these communication systems. Paterson's[12] result shows that the decoherence effect of atmospheric turbulence on a communication system is important, even for weak turbulence. Greg and Robert's research also show that the topological charge of vortex beam is a robust quantity that can be used as an information carrier in optical communications. But the loss of topological charge may occur more rapidly in stronger turbulence.[13] So the propagation properties of a vortex beam in atmospheric turbulence are very important for the system design and application performance estimation. In recent years, a great deal of attention has been paid to the properties of vortex beams in the atmosphere.[13–23] It has been demonstrated that atmospheric turbulence has a great influence on the topological charge, polarization, and intensity distribution of a vortex beam.

A Gaussian vortex beam is a kind of vortex beam that is easy to generate in a laboratory and in a real application system. The optical field of a Gaussian vortex beam can be described by adding a vortex phase to the TEM_{00} Gaussian beam and the eye of the vortex is located at the beam optical axis. However, the short-term intensity pattern and the wander of the beam centroid of this vortex beam have not be studied so far. There has been no quantificational analysis about how the intensity hole varies as the turbulence strength and topological charge change. In this paper, the beam spreading and wandering properties of Gaussian vortex beams are investigated quantitatively by using numerical simulation. The intensity distribution and the dependence of energy hole diameter on the topological charge are discussed. How the topological charge affects the wandering of the beam centroid is analyzed for the first time.

2. Basic parameters of the Gaussian vortex beam and numerical simulation method

According to the definition of the Gaussian vortex beam, the initial optical field of a Gaussian vortex beam could be described as

$$E(x,y,z=0) = E_0(x,y,z=0)\cdot\exp[\mathrm{i}m\theta], \tag{1}$$

where $E_0(x,y,z=0)$ is the optical field of a Gaussian beam field of TEM_{00}, m is the topological charge of vortex phase,

*Project supported by the National Natural Science Foundation of China (Grant No. 61107066).

†Corresponding author. E-mail: qianxianmei@aiofm.ac.cn

© 2015 Chinese Physical Society and IOP Publishing Ltd

and θ is the angular coordinate of the point (x, y). For the collimated Gaussian vortex beam, E_0 can be expressed as

$$E_0(x,y,z=0) = A\exp\left[-\left(x^2+y^2\right)/W_0\right], \tag{2}$$

where A is a constant parameter that is determined by the optical source power and W_0 is initial beam radius.

The optical intensity distribution of a Gaussian vortex beam is the same as that of a Gaussian beam without vortex phase. The phase of a collimated Gaussian vortex beam has a helix distribution. Figure 1 shows the initial phase distributions of collimated Gaussian vortex beams with different topological charges.

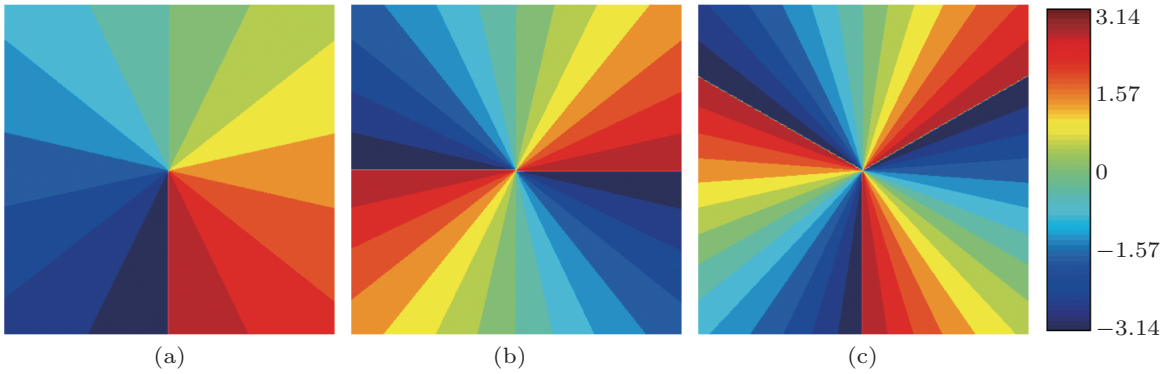


Fig. 1. (color online) Initial phase distributions of collimated Gaussian vortex beams with different topological charges: $m = 1$ (a), 2 (b), and 3 (c).

The numerical simulation of Gaussian vortex beam propagating in atmospheric turbulence is based on the Maxwell wave equation. According to the parabolic approximation of laser beam propagation, the optical filed of laser beam propagation in turbulence satisfies

$$2\mathrm{i}k\frac{\partial E}{\partial z} + \nabla_\perp^2 E + 2k^2 n_1 E = 0, \tag{3}$$

where $k = 2\pi/\lambda$ is the wave number, λ is the wavelength, $n_1 = n - 1$ is the variation of the index of refraction, with n being the refractive index of atmosphere. The multi-phase screen and Fourier transform method[24] is widely used to solve Eq. (1) and to realize the dynamic propagation of an optical wave beam. The extended turbulent random atmosphere is divided into N_s slabs each with a thickness of Δz. For a homogeneous atmospheric path, the medium may be modeled by identical spaced phase screens. So the distance between two phase screens is $\Delta z = L/N_\mathrm{s}$. The phase variation due to the turbulence of each phase screen is $S(x,y,\Delta z) = k\int_{z_{i-1}}^{z_i} n_1(x,y,z)\,\mathrm{d}z$ $(\Delta z = z_i - z_{i-1})$ and the phase spectrum Φ_S can be described by

$$\Phi_\mathrm{S}(\kappa_x,\kappa_y) = 2\pi k^2 \Delta z \Phi_n(\kappa_x,\kappa_y,\kappa_z=0), \tag{4}$$

where Φ_n is the spectrum of the refractive index of the atmosphere, and κ_x and κ_y are the wavenumbers. For a Kolmogorov turbulence, $\Phi_n = 0.033C_n^2\kappa^{-11/3}$, with $\kappa = \sqrt{\kappa_x^2+\kappa_y^2+\kappa_z^2}$. The optical field at position z_i can then be calculated by using

$$E(z,y,z_i) = F^{-1}\left\{\exp\left[-\frac{\mathrm{i}\Delta z}{2k}(\kappa_x^2+\kappa_y^2)\right]F \times\left[\mathrm{e}^{\mathrm{i}S(x,y,\Delta z)}E(x,y,z_{i-1})\right]\right\}, \tag{5}$$

where F and F^{-1} are the Fourier transform and the inverse Fourier transform, respectively.

After obtaining the final optical filed $E(x,y,z=L)$ on the objective plane, the beam properties can be analyzed statistically, such as the spreading of the beam radius, the wandering of the beam centroid, and the intensity distribution structure. The parameters of the beam wave and numerical simulation are chosen to be $\lambda = 1$ μm, $W_0 = 60$ mm, $L = 1$ km, $\Delta x = 1$ mm, $N = 256$, where L is the propagation distance, Δx is the grid interval, and $N \times N$ is the grid number in the simulation phase screen. In this paper, the propagation paths involved are all homogeneous paths, and the turbulent spectrum is assumed to be Kolmogorov spectrum.

3. Intensity-hole effect

Set the values of the structure constant C_n^2 of the refractive index of a homogeneous path to be 5×10^{-16} $\mathrm{m}^{-2/3}$, 1×10^{-14} $\mathrm{m}^{-2/3}$, 5×10^{-14} $\mathrm{m}^{-2/3}$, and 1×10^{-13} $\mathrm{m}^{-2/3}$, respectively, the values of Rytov index β_0^2 are 0.017, 0.332, 1.658, and 3.315, respectively, and choose the topological charge to be $m = 1$. The Rytov index is an integral parameter of C_n^2 and propagation distance L. As to a plane wave, β_0^2 is defined as $\beta_0^2(L) = 4\times0.5631k^{7/6}\int_0^L C_n^2(z)(L-z)^{5/6}\mathrm{d}z$, and for a homogeneous propagation path $\beta_0^2(L) = 1.23k^{7/6}L^{11/6}C_n^2$, where β_0^2 is always introduced to define the fluctuation condition of atmospheric turbulence: $\beta_0^2 > 1$ indicates a strong turbulence, $\beta_0^2 < 1$ indicates a weak turbulence, and $\beta_0^2 \approx 1$ indicates a critical turbulence condition.

Figure 2 displays the corresponding short-term intensity patterns with different C_n^2. It can be seen that there is an in-

tensity hole in the beam center in the presence of a vortex phase. (In the absence of the vortex phase the intensity pattern tends to be a Gaussian distribution, approximately.) In a weak turbulence, the intensity hole can be seen clearly. But as turbulence strength becomes stronger, the margin of the intensity hole becomes blurry and the disturbance of atmospheric turbulence gradually fills that hole. In Fig. 2(d), the intensity pattern breaks up and the intensity hole almost disappears.

The filling effect can be seen more clearly in the long-term intensity patterns. Figure 3 shows the corresponding long-term intensity patterns, which are averaged over 500 short-term intensity patterns.

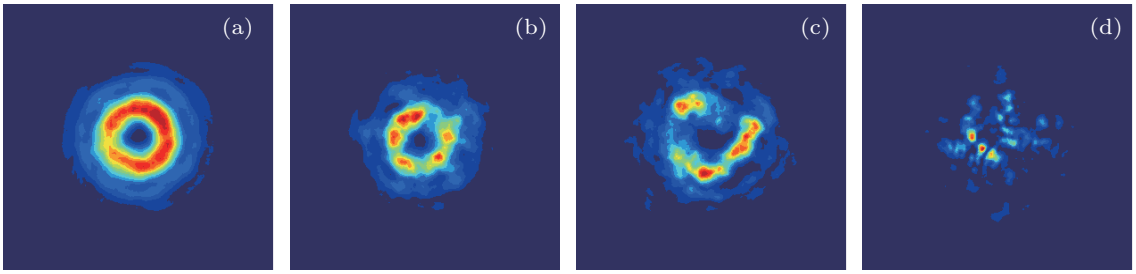


Fig. 2. (color online) Short-term intensity patterns with different turbulence strengths: $\beta_0^2 = 0.017$ (a), 0.332 (b), 1.658 (c), and 3.315 (d).

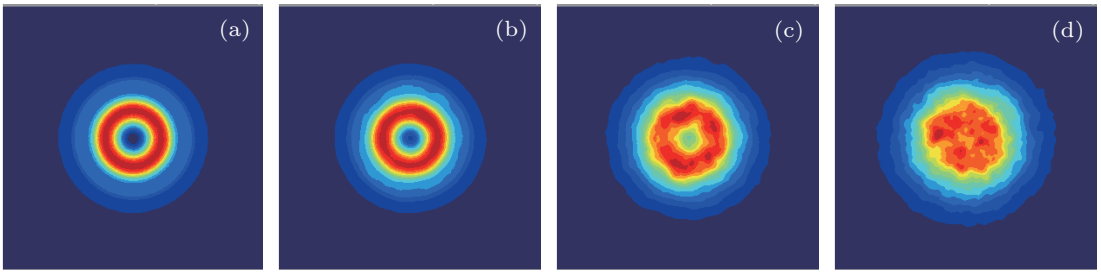


Fig. 3. (color online) Long-term intensity patterns with different turbulence strength: $\beta_0^2 = 0.017$ (a), 0.332 (b), 1.658 (c), and 3.315 (d).

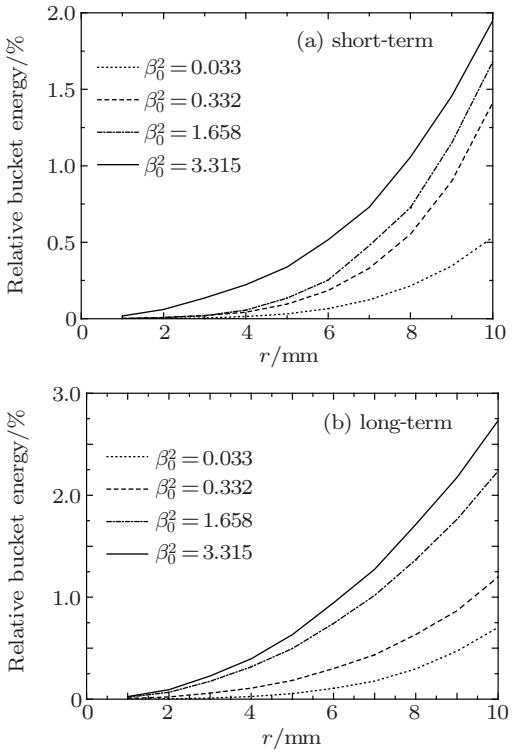


Fig. 4. Relative bucket energies in a disk versus disk radius and turbulence strength: short-term and (b) long-term.

The size of the intensity hole and its variation in the atmosphere are important for analyzing the effect of the vortex phase on the vortex beam propagation. We calculate the energy contained in a specific disk with radius r, namely bucket energy, which is shown in Fig. 4. The energy is normalized to the power of the beam source, so we call it relative bucket energy. The long-term patterns involved in Fig. 4(b) are averaged over 1000 short-term intensity patterns. It can be seen that there is almost no energy for $r < 4$ mm when $\beta_0^2 = 0.033$. And as the turbulence strength turns stronger, the intensity hole is gradually filled by energy. However, the relative bucket energy is also less than 2.5%, even in a strong turbulence for $r < 10$ mm.

We calculate the relative bucket energy $P_{10\ \mathrm{mm}}$ in a disk for radius $r = 10$ mm as a function of Rytov index β_0^2 with topological charges: $m = 0$, $m = 1$, and $m = 2$, respectively, which is shown in Fig. 5. We can see that for a Gaussian beam with no vortex phase ($m = 0$) the relative bucket energy tends to decline as turbulence turns stronger, which happens because of the beam spreading due to atmospheric turbulent effects. For Gaussian vortex beams ($m = 1$ and $m = 2$) the relative bucket energy increases from a very small value to the peak value as the turbulence turns from weak to strong. This indicates that atmospheric turbulence has the effect or ability to fill the intensity hole. It can also be seen that for larger topolog-

ical charge the relative bucket energy $P_{10\ \mathrm{mm}}$ may be smaller. When $\beta_0^2 = 1.989$ the relative energies are 4.2%, 2.5%, and 1.4% for $m = 0$, 1, 2, respectively.

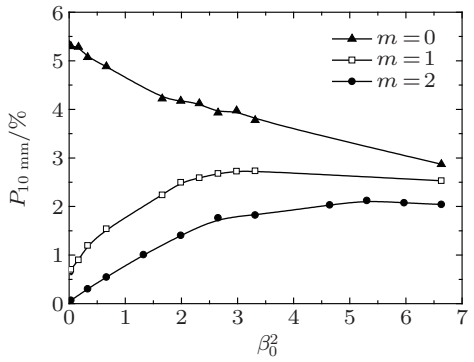


Fig. 5. Plots of relative bucket energy $P_{10\ \mathrm{mm}}$ versus turbulence strength with different topological charges.

We assume the radius $R_{5\%}$ which contains 5% of the total energy to be the radius of the intensity hole of a vortex beam propagating in the atmosphere. Figure 6 shows plots of the $R_{5\%}$ of long-term intensity patterns versus turbulence strength with topological charges $m = 1$ and $m = 2$. It can be seen that $R_{5\%} = 17.0$ mm and $R_{5\%} = 22.8$ mm, respectively, for $m = 1$ and $m = 2$ when there is no atmospheric turbulence. These two radii are very large, which contain only 5% of the total energy, indicating that the intensity–hole effect of vortex beam is very serious when propagating in a vacuum. However, $R_{5\%}$ declines quickly as the turbulence becomes strong. This happens because the disturbance of atmospheric turbulence has the ability to fill the intensity hole with optical energy. As the turbulence strength continues to become strong, there exists a minimum value of $R_{5\%}$, and then $R_{5\%}$ tends to rise because of the serious beam spreading due to strong atmospheric turbulent effects.

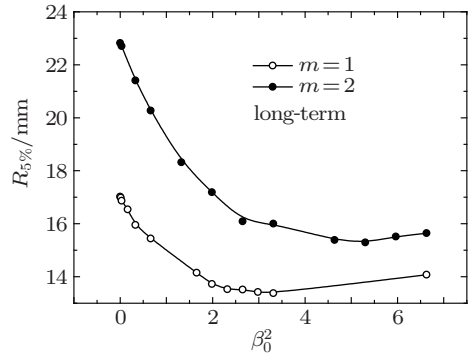


Fig. 6. Plots of $R_{5\%}$ versus turbulence strength for $m = 1$ and $m = 2$.

4. Beam spreading and wandering

We use the effective beam radius to describe the beam spreading of a vortex beam propagating in spite of the existence of an energy hole. The effective radius can be expressed by

$$W_{\mathrm{eff}}^2 = \sqrt{2}\iiint r^2 I(x,y)\,\mathrm{d}x\mathrm{d}y \Big/ \iint I(x,y)\,\mathrm{d}x\mathrm{d}y, \tag{6}$$

where $I(x,y)$ is the intensity distribution. Figure 7 displays the short-term and long-term effective beam radii of vortex beams versus turbulence strength with different topological charges. We can see that the effective radius of a vortex beam with larger topological charge is greater than with a smaller topological charge. The beam spreading of the vortex beam may due to two reasons: the intensity-hole effect and the turbulent effect. Although a strong turbulent effect can fill the intensity hole with energy, the spreading of the vortex beam is also larger than that with no vortex phase. This can also be seen from Fig. 5.

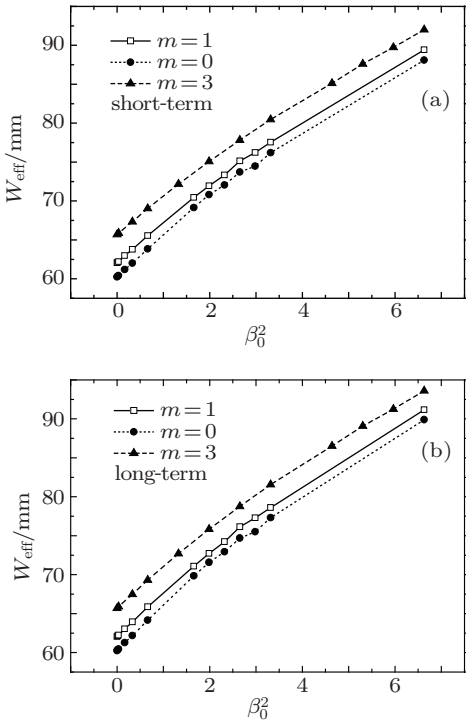


Fig. 7. Plots of short-term (a) and long-term (b) effective beam radii of vortex beams versus turbulence strength with different topological charges.

The wandering of the beam centroid is defined by the beam wander variation, which can be described by the following expression:

$$\sigma_\rho^2 = \iiiint (\boldsymbol{\rho}_1 \cdot \boldsymbol{\rho}_2) I(\boldsymbol{\rho}_1) I(\boldsymbol{\rho}_2)\,\mathrm{d}\boldsymbol{\rho}_1\,\mathrm{d}\boldsymbol{\rho}_2 \Big/ \left[\iint I(\boldsymbol{\rho})\,\mathrm{d}\boldsymbol{\rho}\right]^2, \tag{7}$$

where $I(\boldsymbol{\rho})$ is the intensity distribution. The centroid $(x_\mathrm{c}, y_\mathrm{c})$ of the beam pattern can be expressed by

$$\begin{aligned} x_\mathrm{c} &= \iint x I(x,y)\,\mathrm{d}x\mathrm{d}y \Big/ \iint I(x,y)\,\mathrm{d}x\mathrm{d}y, \\ y_\mathrm{c} &= \iint y I(x,y)\,\mathrm{d}x\mathrm{d}y \Big/ \iint I(x,y)\,\mathrm{d}x\mathrm{d}y. \end{aligned} \tag{8}$$

The beam wander variation can then be expressed as

$$\sigma_\rho^2 = \sigma_{x\mathrm{c}}^2 + \sigma_{y\mathrm{c}}^2, \tag{9}$$

where σ_{xc}^2 and σ_{yc}^2 are the variations of x_c and y_c, respectively.

Figure 8 displays the RMSs of beam wander variation as a function of turbulence strength with different topological charges. It shows that topological charge has no evident influence on beam wandering and beam wander variations of vortex beams of different topological charges are almost equal to those of a Gaussian beam with no vortex phase.

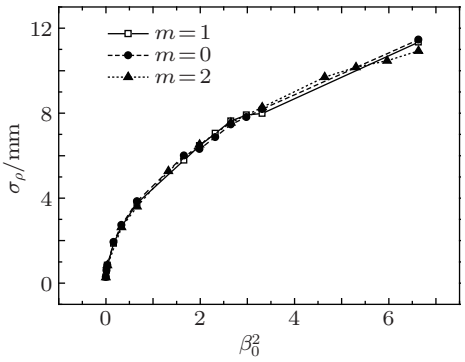


Fig. 8. Plots of beam wander variance versus turbulence strength with different topological charges.

5. Conclusions

The propagation properties of Gaussian vortex beam are quietly different from those of a Gaussian beam without a vortex phase. We use wave optics numerical simulation to study the intensity pattern, beam spreading, and wandering properties of a Gaussian vortex beam propagating in a turbulent atmosphere. The differences in propagation properties between a Gaussian vortex beam and a Gaussian beam are analyzed. The results show that in the center of beam pattern an intensity hole appears gradually as the Gaussian vortex beam propagates. The size of the intensity hole increases with the increase of topological charge but decreases with the growth of turbulence strength. This happens because the intensity hole could be filled with optical energy by the disturbance of atmospheric turbulence to some extent. The spreading of the Gaussian vortex beam is more serious than that of the Gaussian beam. However, the beam wander of Gaussian vortex beam is almost the same as that of the Gaussian beam. The vortex phase structure has no evident influence on beam wandering. All of these properties of the vortex beam can provide some theoretical base for the application of a vortex beam in free space communications, especially for intensity receival and detection.

References

[1] Ponomarenko S A 2001 *J. Opt. Soc. Am. A* **18** 150
[2] Bogatyryova G V, Fel'de C V and Polyanskii P V 2003 *Opt. Lett.* **28** 878
[3] Dijk T V and Visser T D 2009 *J. Opt. Soc. Am. A* **26** 741
[4] Chen B S, Zhang Z M and Pu J X 2009 *J. Opt. Soc. Am. A* **26** 862
[5] Allen L, Bejersbergen M W, Spreeuw R J C and Woerdman J P 1992 *Phys. Rev. A* **45** 8185
[6] Soskin M S, Gorshkov V N and Vasnetsov M V 1998 *Phys. Rev. A* **56** 4064
[7] Vickers J, Burch M, Vyas R and Singh S 2008 *J. Opt. Soc. Am. A* **25** 823
[8] Zhou Z H, Guo Y K and Zhu L Q 2014 *Chin. Phys. B* **23** 044201
[9] Luo Y M, Gao Z H, Tang B H and Lv B D 2014 *Acta Phys. Sin.* **63** 154201 (in Chinese)
[10] Gahagan K T and Swartzlander G A 1999 *J. Opt. Soc. Am. B* **16** 533
[11] He H, Friese M E J, Heckenberg N R and Rubinsztein-Dunlop H 1995 *Phys. Rev. Lett.* **75** 826
[12] Paterson C 2005 *Phys. Rev. Lett.* **94** 153901
[13] Greg G and Robert K T 2008 *J. Opt. Soc. Am. A* **25** 225
[14] Vinotte A and Berg L 2005 *Phys. Rev. Lett.* **95** 193901
[15] Ramee S and Simon R 2000 *J. Opt. Soc. Am. A* **17** 84
[16] Cheng W, Haus J W and Zhan Q W 2009 *Opt. Express* **17** 17829
[17] Cheng K, Yan H W and Lv B D 2008 *Acta Phys. Sin.* **57** 4911 (in Chinese)
[18] Wang T, Pu J X and Rao L Z 2007 *Opt. Tech.* **33** 4 (in Chinese)
[19] Yan H W, Cheng K and Lv B D 2008 *Acta Phys. Sin.* **57** 5542 (in Chinese)
[20] Chen Z Y, Zhang G W, Rao L Z and Pu J X 2008 *Chin. J. Lasers* **35** 1063
[21] Rao L Z and Pu J X 2007 *J. Opt. Soc. Am. A* **24** 2242
[22] Zhu K C, Zhou G Q, Li X G, Zheng X J and Tang H Q 2008 *Opt. Express* **16** 21315
[23] Shu J H, Chen Z Y and Pu J X 2009 *Chin. Phys. Lett.* **26** 024207
[24] Knepp D L 1983 *Proc. IEEE* **71** 722